

Influence of Shape of nanoparticle on flow and heat transfer of nanofluid in the presence of joule heating along a stretching surface

Syed Wajeed-Ul-Hussan, Azeem Shahzad
syedwajeedulhussan174@gmail.com, azeem.shahzad@uettaxila.edu.pk

Abstract

The main objective of this numerical work is to investigate the effects of slip condition and Joule heating on the two-dimensional incompressible magneto hydrodynamic convection flow of a nanofluid across a stretched sheet in a steady state. The nanofluid under investigation is a solution of water and silver nanoparticles. The nonlinear governing system of equations is simplified by similarity transformation and is then numerically solved in MATLAB using the BVP4C. Graphs are used to show the effects of the slip, magnetic, Joule heating, and volume fraction parameters on temperature and velocity. Tabular estimates are also provided for physical parameters such as the skin friction coefficient and Nusselt number. It is observed from the results that incrementing the magnetic parameter and volume fraction values results in enhancement of skin friction, while opposite trend seen for slip parameter. Increasing the values of magnetic parameter, slip parameter, Eckert number and volume fraction results in decay of Nusselt number.

Keywords: Stretching surface, Magneto hydrodynamic (MHD), Silver Ag nanoparticles.

Date of Submission: 25-05-2024

Date of acceptance: 05-06-2024

I. INTRODUCTION

A suspension of nanoparticles (ranges between 1 to 100 nm) in a base fluid, such as water, alcohol, oil, or ethylene glycol, is known as a nanofluid. Over the last few decades, nanofluid has attracted a lot of interest of researchers due to its application in the fields of thermal engineering, nanotechnology, and various other applications. Recently, some researchers have suggested and investigated the use of nanofluid technology to manage heat transfer in a process using experiments or numerical analysis. Applications for the nanofluid include heat exchangers, electronic equipment cooling, chemical reactions, oil purification, fiber manufacture, plastic and rubber sheeting, and lubrication. Furthermore, one of the greatest operational tactics for efficiently controlling the temperature of a range of mechanical and industrial systems, such as generators, is to convert from traditional fluids to nanofluid. Choi [1] is credited with introducing the concept of nanofluid to improve thermal performance. J. A. Eastman [2] examine the effect of thermal conductivity of mixtures of fluids and nanometer-size particles is measured by a steady-state parallel-plate method. An analytical investigation is conducted by S. Nadeem [3] on the steady boundary layer flow of nanofluid over an exponential stretching surface. K. Rafique [4] examine the impact of NP shape on the entropy generated by an $Al_2O_3 - H_2O$ nanofluid on a permeable MHD stretching sheet when heat radiation, viscous dissipation, and quadratic velocity are present.

H_2O is the cold fluid, and $Al_2O_3 - H_2O$ nanofluid is the hot fluid. It consists of five different NP forms: oblate spheroid, platelet, blade, brick, and cylinder. S. Bibi [5] explain the heat transfer and unsteady film flow of a SiO_2 water nanofluid across a stretching sheet with convective boundary conditions. K. Sharma [6] studies the steady two-dimensional flow of an incompressible magneto hydrodynamics (MHD) boundary layer in the presence of thermal radiation and viscous dissipation, as well as the heat transfer of a nanofluid over an impermeable barrier. And many other scientist work on nanofluid.

Silver nanomaterial possess unique physical, chemical, and optical properties, attracting interest for their antimicrobial properties. Their strong coupling to specific light wavelengths allows for tunable optical responses, making them useful in developing ultra-bright reporter molecules, thermal absorbers, and nano-scale antennas. The precise engineering of silver nanoparticle size and shape is crucial for various applications. A MHD flow of Ag water nanofluid across a flat porous plate was examined by Upreti [7]. Esfe [8] carried out tests to determine the thermal conductivity and dynamic viscosity of $Ag - MgO$ /water hybrid nanofluids. An extensive article on the thermophysical characteristics of $Al_2 - Nps$ was provided by Timofeeva [9]. T. Hayat [10] talked about using a hybrid nanofluid of $AgCuO$ and water to improve heat transmission. Godson

[11] provided an experimental analysis of the viscosity and thermal conductivity of silver water

nanofluid. Rashid [12] studied the impact of nanoparticle shape on Al₂O₃-Water nanofluid flow and heat transfer over a stretching sheet. Scholars [13]–[20] have studied nano-particles' effects in different geometries, including silver nanoparticles dispersed in ethylene glycol, Ag water nanofluid flow over a porous plate, Ag-MgO/water hybrid nanofluids thermal conductivity and dynamic viscosity, Al₂ – Nps thermophysical properties, heat transfer enhancement with Ag –CuO/water hybrid nanofluid, and water-Ag nanofluid fertilization efficiency in thermal systems.

Rapid advancements in a number of scientific and technological domains have compelled researchers to broaden their focus to include the regime of boundary layer flow over a stretching sheet. Boundary layer flow behavior toward a linearly or nonlinearly stretching sheet is important for solving engineering problems and has many applications in manufacturing and production processes, such as wire drawing, extrusion of polymer sheets, glass fiber production, rubber sheet manufacturing, metal spinning, petroleum industries, and polymer processing, among many others. Using a convective boundary condition, D. Srinivasacharya [21] examines the effects of Joule heating on the viscous fluid flow over a porous sheet that is stretching exponentially. As the appearance of Joule heating occurs, N. S. Khashi'ie [22] examine the flow and heat transfer of the hybrid nanofluid past a shrinking cylinder while keeping an eye on the duality of solutions. S. Riaz

[23] examine the effects of slip condition, Joule heating, and viscous dissipation on the steady, incompressible, two-dimensional magneto hydrodynamic convection flow of a nanofluid across a stretched sheet. The impact of Joule heating and Lorenz force on MHD natural convection and entropy formation within a lid-driven cavity filled with Fe₃O₄-water nanofluid has been investigated numerically by O. Ghaffarpassand [24]. In the presence of nonlinear thermal radiation,

K. Ganesh Kumar [25] examines the combined effects of viscous dissipation and Joule heating on the three-dimensional flow and heat transfer of a Jeffrey nanofluid. N. S. Khashi'ie [26] investigates the Joule heating and MHD hybrid nanofluid flow with heat transmission on a movingplate.

This article investigates steady heat transfer and flow in Ag nanoparticles with added effects like thermal radiation, joule heating, magneto-hydrodynamic (MHD), velocity slip, and convective boundary conditions over time independent stretching surfaces. It is the first study to investigate steady heat transfer and flow over time dependent stretching surface with water as the base liquid. Here we use a Cartesian coordinate system for mathematical formulation and solve the simplified nonlinear ODEs system using an efficient convergent method (BVP4C). The calculations are performed using MATLAB software. Also included graphs to explain the impact of physical parameters on velocity, temperature, skin fraction number and Nusselt number.

NOMENCLATURE

ϕ	Solid volume fraction	E_c	Eckert number
μ_f	Dynamic viscosity of base fluid	ρ_f	Density of base fluid
k_f	Thermal conductivity of base fluid	ρ_s	Density of nanoparticles
k_{nf}	Thermal conductivity of nanofluid	μ_{nf}	Viscosity of nanofluid
$(\rho C_p)_{nf}$	Heat capacitance of nanofluid	ρ_{nf}	Density of nanofluid
S	Unsteadiness parameter	Pr	Prandtl number
M	Magnetic Parameter	K	Slip Parameter
η	Similarity Variable	Re	Reynolds number
Ψ	Stream function	C_f	Skin friction coefficient

PROBLEM FORMULATION

Examine the flow of two-dimensional boundary layers across a steady stretched surface containing Ag-nanoparticles in different shapes with joule heating. A constant magnetic field with strength B_o is applied perpendicular to the flow. The mathematical model in the form of partial differential equations will be transformed into ordinary differential equations using similarity transformations. Next, an analytical solution to the ordinary differential equations will be provided. In this case, the y-axis is normal to the x-axis, and the x-

axis is chosen in the direction of the sheet motion. Let $T = T(x, y)$ be the temperature of the nanofluid and let $u = u(x, y)$ and $v = v(x, y)$ be the components of velocity along the coordinate axis. Allow the base fluid (water) and multi-shape nanoparticles to be thermally balanced as well.

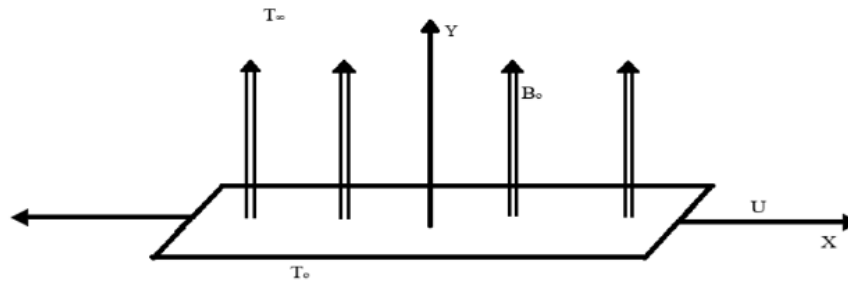


Figure 1. Graphical representation of the modelled problem.

Continuity, momentum and energy equation [5]

$$\frac{\partial u}{\partial x} + \frac{\partial v}{\partial y} = 0 \quad (1)$$

$$u \frac{\partial u}{\partial x} + v \frac{\partial v}{\partial y} = \frac{\mu_{nf}}{\rho_{nf}} \frac{\partial^2 u}{\partial y^2} - \frac{\sigma_{nf} B(t)^2 u}{\rho_{nf}} \quad (2)$$

$$u \frac{\partial T}{\partial x} + v \frac{\partial T}{\partial y} = \frac{k_{nf}}{(\rho C_p)_{nf}} \frac{\partial^2 T}{\partial y^2} + \frac{\mu_{nf}}{(\rho C_p)_{nf}} \left(\frac{\partial u}{\partial y} \right)^2 + \frac{\sigma_{nf} B(t)^2 u^2}{(\rho C_p)_{nf}} \quad (3)$$

Subject to the boundary conditions [5], [27]

$$u = U + A v_f \frac{\partial u}{\partial y}, \quad v = 0, \quad T = T_w = T_\infty + A_0 \left(\frac{x}{l} \right)^2, \quad \text{at} \quad y = 0,$$

$$U \rightarrow 0, \quad T \rightarrow T_\infty, \quad \text{as} \quad y \rightarrow \infty$$

Physical parameters [28]

$$\text{Where } \alpha_{nf} = \frac{K_{nf}}{(\rho C_p)_{nf}}, \quad \rho_{nf} = (1 - \phi) \rho_f + \phi \rho_s,$$

$$\frac{\mu_{nf}}{\mu_f} = (1 + A_1 \phi + A_2 \phi^2), \quad \frac{\sigma_{nf}}{\sigma_f} = (1 - \phi) \sigma_f + \phi \sigma_s$$

And thermal conductivity ratio is

$$\frac{k_{nf}}{k_f} = \frac{K_s + (m - 1) \cdot k_f + (m - 1)(k_s - k_f) \cdot \phi}{k_s + (m - 1) \cdot k_f - (k_s - k_f) \cdot \phi}$$

Using similarity transformation [29] mentioned below, we will obtain dimensionless variables, which will be utilized to make the system dimensionless.

$$\psi = xuRe^{-1/2}f(\eta), \quad \eta = \frac{y}{x}Re^{1/2}, \quad \theta(\eta) = \frac{T-T_{\infty}}{T_w-T_{\infty}} \quad (4)$$

Here ψ is the stokes theorem function and η will be independent variable,

$$u = \frac{\partial\psi}{\partial x} \quad \& \quad v = -\frac{\partial\psi}{\partial y}$$

Thus velocity components developed as

$$u = U f'(\eta), \quad v = -\left(\frac{bv_f}{1-\alpha t}\right)^{\frac{1}{2}} f(\eta) \quad (5)$$

Equations (2) and (3) are transformed into a set of ordinary differential equations (ODE) with boundary conditions using the collection of similarities discovered.

$$\varepsilon_1 f''' - f'^2 + ff'' - \varepsilon_3 M f' = 0, \quad (6)$$

$$\theta''(\eta) + \frac{Pr}{\varepsilon_2} (-2f'\theta(\eta) + f\theta'(\eta) + \varepsilon_4 Ec f''^2 + \varepsilon_5 Ec M f'^2) = 0 \quad (7)$$

Boundary conditions are

$$\left. \begin{aligned} f(0) = 0, \quad f'(0) = 1 + K \cdot f''(0), \\ f'(\infty) = 0, \quad \theta(0) = 1, \quad \theta(\infty) = 0 \end{aligned} \right\} \quad (8)$$

Here $\varepsilon_1, \varepsilon_2, \varepsilon_3, \varepsilon_4$ & ε_5 are three constants which are defined as

$$\varepsilon_1 = \frac{1 + A_1 \phi + A_2 \phi^2}{\left(1 - \phi + \phi \cdot \left(\frac{\rho_s}{\rho_f}\right)\right)}, \quad \varepsilon_2 = \frac{\frac{k_{nf}}{k_f}}{\left(1 - \phi + \phi \cdot \left(\frac{(\rho c_p)_s}{(\rho c_p)_f}\right)\right)}, \quad \varepsilon_3 = \frac{\left(1 - \phi + \phi \cdot \left(\frac{\sigma_s}{\sigma_f}\right)\right)}{\left(1 - \phi + \phi \cdot \left(\frac{\rho_s}{\rho_f}\right)\right)},$$

$$\varepsilon_4 = \frac{\left(1 - \phi + \phi \cdot \left(\frac{\sigma_s}{\sigma_f}\right)\right)}{\left(1 - \phi + \phi \cdot \left(\frac{(\rho c_p)_s}{(\rho c_p)_f}\right)\right)}, \quad \varepsilon_5 = \frac{1 + A_1 \phi + A_2 \phi^2}{\left(1 - \phi + \phi \cdot \left(\frac{(\rho c_p)_s}{(\rho c_p)_f}\right)\right)},$$

$$C_f Re^{\frac{1}{2}} = (1 + A_1 \phi + A_2 \phi^2) f''(0), \quad (9)$$

$$Nu Re^{-\frac{1}{2}} = -\frac{k_{nf}}{k_f} \theta'(0) \quad (10)$$

Here, Pr is the Prandtl number, $K = A \sqrt{\frac{\nu_f U_w}{r}}$ partial slip parameter, $Ec = \frac{U^2}{c_p(T_{\infty}-T)}$ is the Eckert number. The constants $\varepsilon_1, \varepsilon_2, \varepsilon_3, \varepsilon_4$ and ε_5 are also present. Equations (9) and (10) are the heat transfer coefficient's skin fraction-coefficient ($C_f Re^{\frac{1}{2}}$) and Nusselt number ($Nu Re^{-\frac{1}{2}}$).

Numerical solution

This article uses the BVP4C [30] technique to get the solution. The main characteristics of the suggested BVP4C technique, which include handling single BVPs, direct acceptance of both two-point and multipoint BVPs with improved accuracy, and faster convergence with reduced error, are well recognized in the research community. The fundamental method of BVP4C is a widely used Simpson's method that may be found in a number of programs. To use the approach, third order ordinary differential equation (6) and second order ordinary differential equation (7) are turned into first order differential equations.

Let us consider,

$$f = y_{(1)},$$

then we can write

$$f' = y'_{(1)} = y_{(2)}, \text{ so}$$

$$f'' = y'_{(2)} = y_{(3)}, \text{ and then 6}^{\text{th}} \text{ \& } 7^{\text{th}} \text{ equation can be written as}$$

$$f''' = y'_{(3)} = \frac{1}{\epsilon_1} * \left((y_{(2)})^2 - y_{(1)} * y_{(3)} + \epsilon_3 * M * y_{(2)} \right), \quad (11)$$

$$\theta = y_{(4)},$$

$$\theta' = y'_{(4)} = y_{(5)}, \text{ and}$$

$$\theta'' = y'_{(5)} = \frac{Pr}{\epsilon_2} * \left(2 y_{(2)} * y_{(4)} - y_{(1)} * y_{(5)} - Ec * \epsilon_4 * (y_{(3)})^2 - \epsilon_5 * Ec * M * (y_{(2)})^2 \right) \quad (12)$$

Boundary conditions are

$$\left. \begin{aligned} y_{(1)}(0) = 0, \quad y_{(2)}(0) = 1 + K * y_{(3)}(0), \\ y_{(2)}(\infty) = 0, \quad y_{(4)}(0) = 1, \quad y_{(4)}(\infty) = 0 \end{aligned} \right\} \quad (13)$$

Table 1: Thermo physical properties [31] of Ag nanoparticle and base fluid.

Nanoparticle/Base water	Thermal conductivity (W/m K)	Density(kg/m ³)	Electric conductivity (S/m)	Specific heat(J/kg K)
Ag	429	10500	63	235
H ₂ O	0.613	997.1	5.50	4179

Table 2: Viscosity and shape factor values of nanoparticle [5].

Nanoparticles	Cylinder	Platelet	Blade	Brick	Sphere
Parameters					
A ₁	13.5	37.1	14.6	1.9	2.5
A ₂	904.4	612.6	123.3	471.4	6.5
m	4.82	5.72	8.26	3.72	3.0

NUMERICAL RESULTS AND DISCUSSION

In this study, we investigate a mathematical model for two-dimensional boundary layer flow of nanofluids with different shapes of Ag nanoparticles. Using similarity transformations, we convert the modeled partial differential equations into ordinary differential equations. Subsequently, we analyze the impact of

various parameters including the magnetic field parameter (M), partial slip condition (K), Eckert number (Ec), Prandtl number (Pr), and nanoparticle volume fraction (ϕ) on both the velocity and temperature profiles within the boundary layer. These effects are visually demonstrated through graphical results presented in figures 2 to 10.

Our study explored the impact of several key parameters on the velocity profile of nanofluids with different nanoparticle shapes, focusing on silver (Ag) nanoparticles. The results are presented visually in figures 2-5. Figures 2(a-e) investigate the effect of the magnetic field parameter (M) on the velocity profile within the boundary layer. As M increases, a noticeable decrease in the velocity of all Ag nanoparticle shapes is observed. This can be attributed to the Lorentz force arising from the interaction between the applied magnetic field and the induced currents in the nanofluid. Figures 3(a-e) illustrate the effect of the partial slip condition (K) on the velocity profile. Interestingly, increasing K also leads to a reduction in velocity for all Ag nanoparticle shapes. This phenomenon can be explained by the reduced momentum transfer at the fluid-wall interface due to the partial slip condition. Figures 4(a-e) delve into the impact of nanoparticle volume fraction (ϕ) on the velocity profile. Notably, increasing ϕ enhances the velocity for most Ag nanoparticle shapes, including cylinders, platelets, blades, and bricks. However, a unique exception is observed for spherical nanoparticles, where increasing ϕ actually leads to a velocity decrease. This contrasting behavior can be attributed to the interplay between various factors such as particle shape, interparticle interactions, and heat transfer mechanisms. Finally, figure 5 provides a fascinating comparison of the velocity profiles for different Ag nanoparticle shapes. We observe that the velocity ranking from highest to lowest is as follows: platelets > cylinders > blades > bricks > spheres. This suggests that platelet-shaped nanoparticles offer the strongest enhancement in nanofluid velocity, while spherical nanoparticles exhibit the least impact.

In our study, we explored not only the influence of parameters on velocity profiles, but also their impact on the thermal behavior of Ag nanofluid flows. Let's dive into the insights revealed by figures 6-10.

Figures 6(a-e) illustrate the exciting interaction between the magnetic field parameter (M) and fluid temperature. Notably, as M increases, we observe a distinct rise in fluid temperature. This phenomenon can be explained by the dissipation of kinetic energy into thermal energy due to the Lorentz force acting on the electrically conducting nanofluid. Figures 7(a-e) illustrate the effect of the partial slip condition (K) on the temperature profile. Interestingly, increasing K also leads to an increase in temperature for all Ag nanoparticle shapes. Figures 8(a-e) delve into the impact of nanoparticle volume fraction (ϕ) on temperature. Interestingly, increasing ϕ generally leads to a temperature increase for most Ag nanoparticle shapes, including cylinders, platelets, blades, and bricks. This can be attributed to enhanced heat generation within the nanofluid due to higher particle concentration. **Figures 9(a-e)** shed light on the role of the Eckert number (Ec) in shaping the temperature profile. As Ec increases, we observe a further enhancement in temperature. This signifies the growing importance of viscous dissipation with increasing fluid velocity. Finally, Figure 10 offers a fascinating comparison of temperature profiles for different Ag nanoparticle shapes. We can discern that the temperature ranking, from highest to lowest, follows the order: platelets, cylinders, blades, bricks and spheres. This suggests that platelet-shaped nanoparticles exhibit the most significant impact on heat generation, while spherical nanoparticles contribute the least. These findings unveil the intricate relationships between various parameters and their influence on the thermal behavior of Ag nanofluids. Such insights can guide the design and optimization of nanofluid-based systems for diverse applications in thermal management, energy harvesting, and beyond.

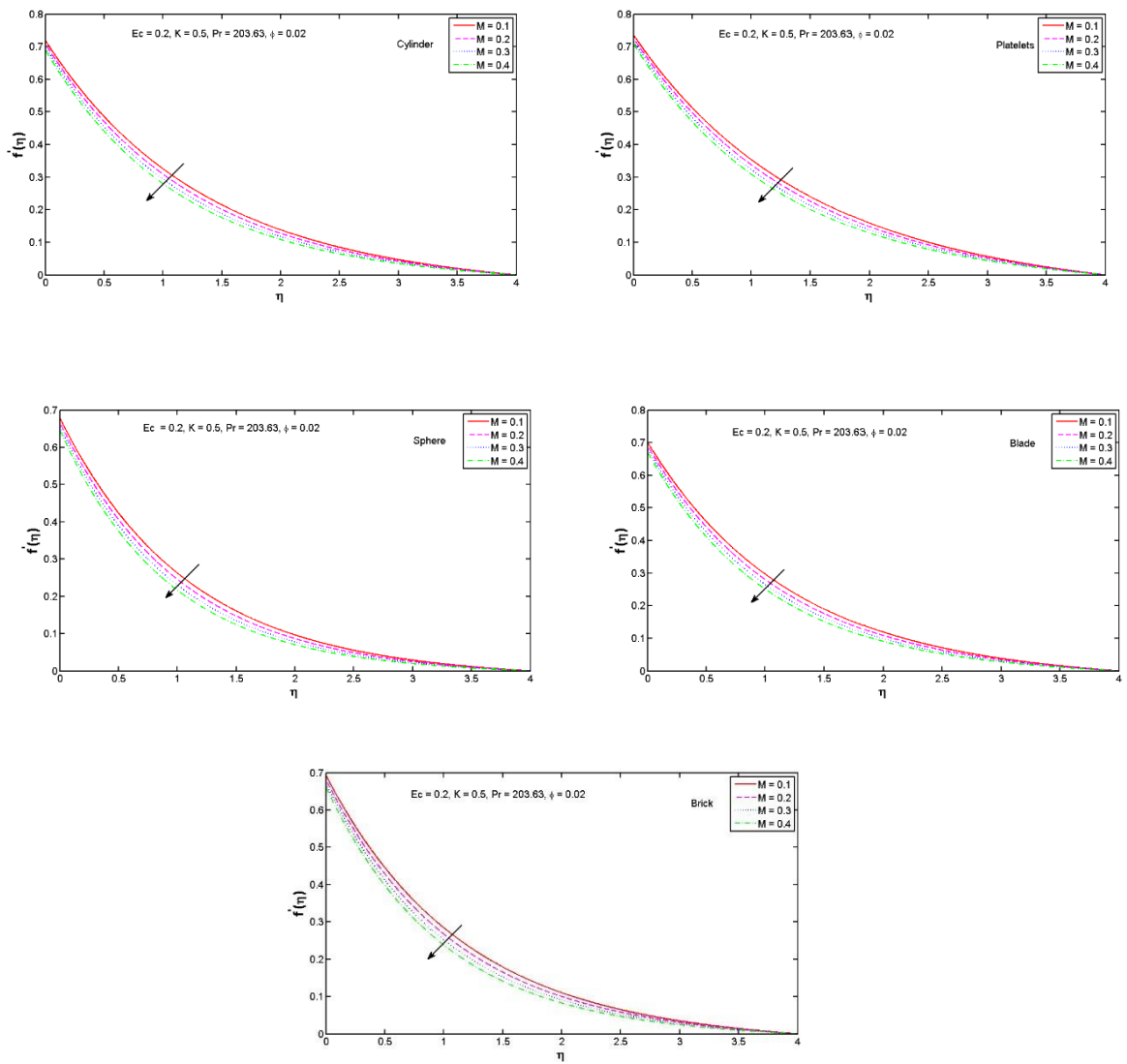


Figure 2(a-e): Impact of magnetic parameter (M) on velocity profile.

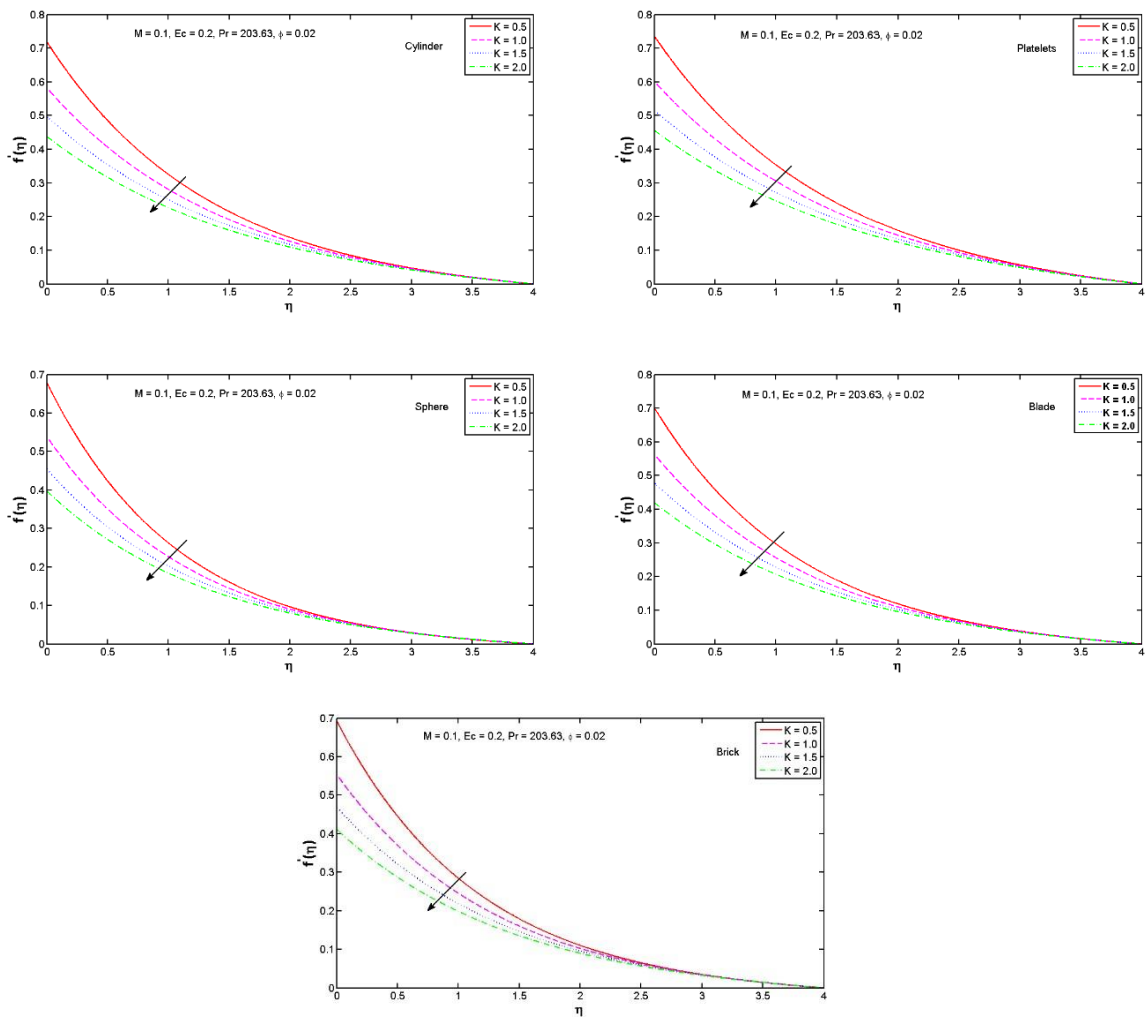


Figure 3(a-e): Outcome of Slip Parameter (K) on Velocity Profile.

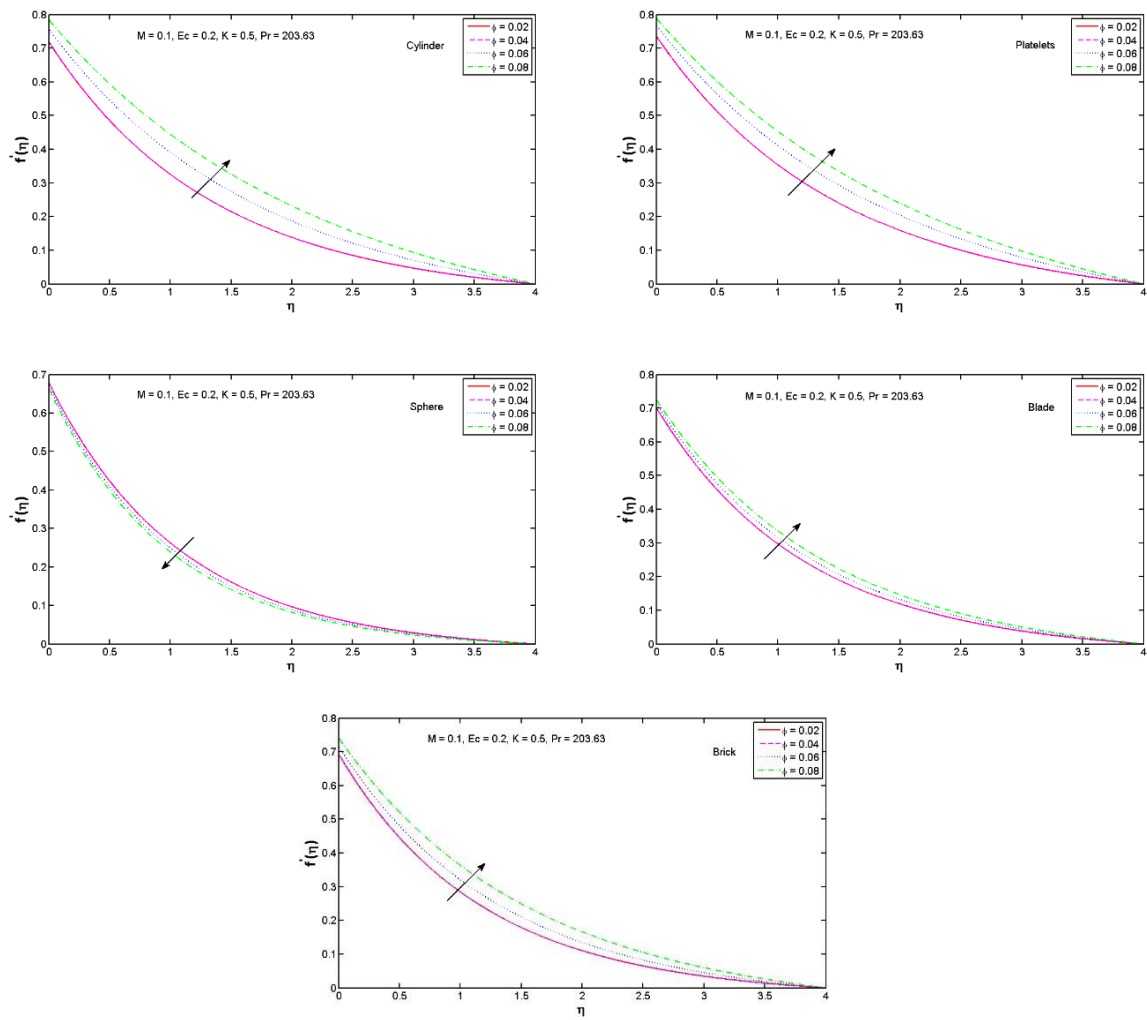


Figure 4(a-e): Influence on Volume Fraction (ϕ) on Velocity Profile.

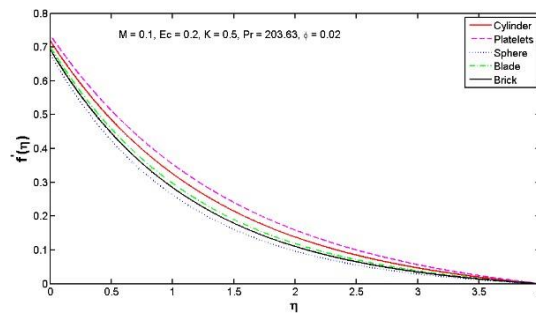


Figure 5. Variation in Velocity profile for Different shapes of nanoparticles.

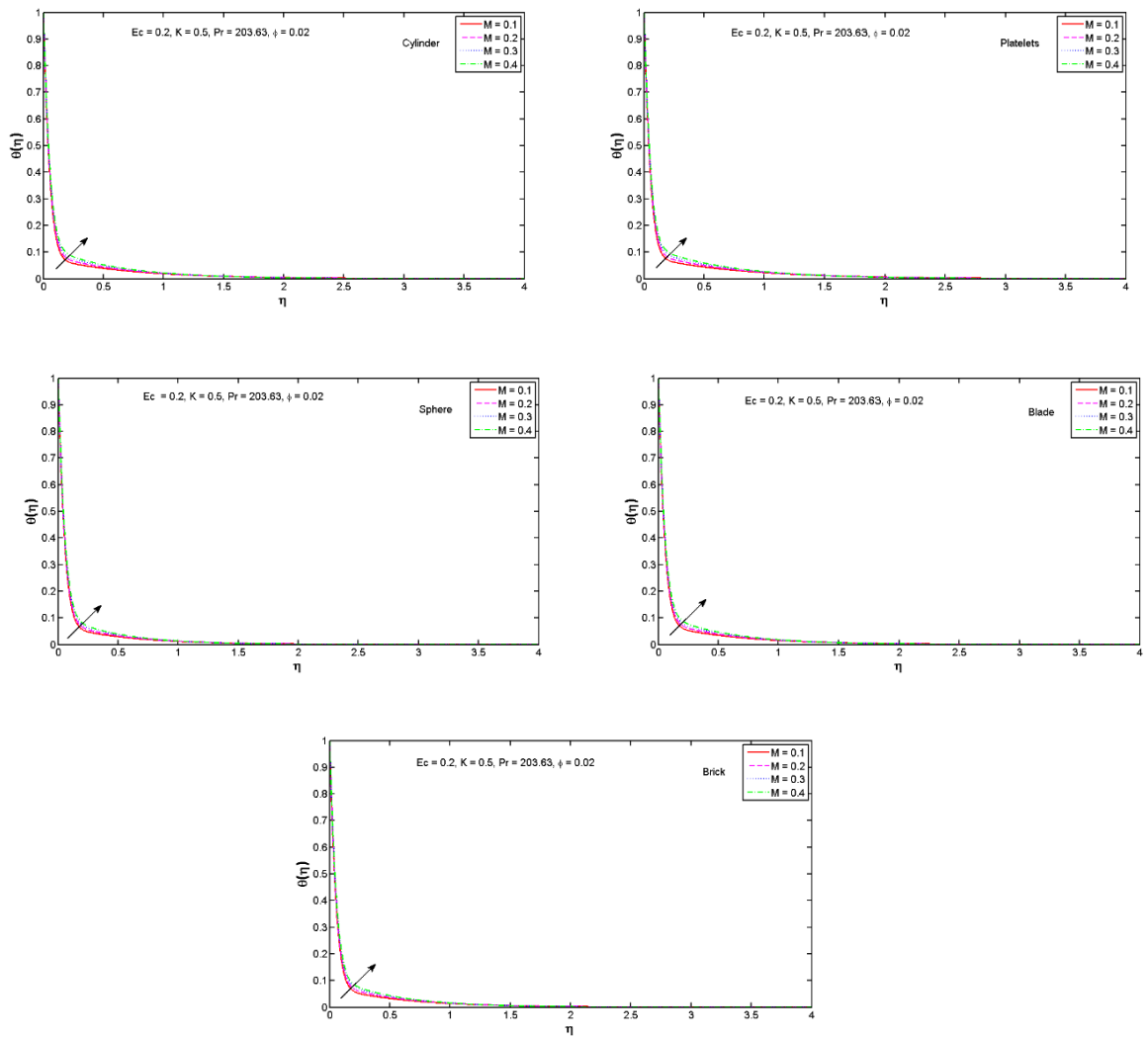
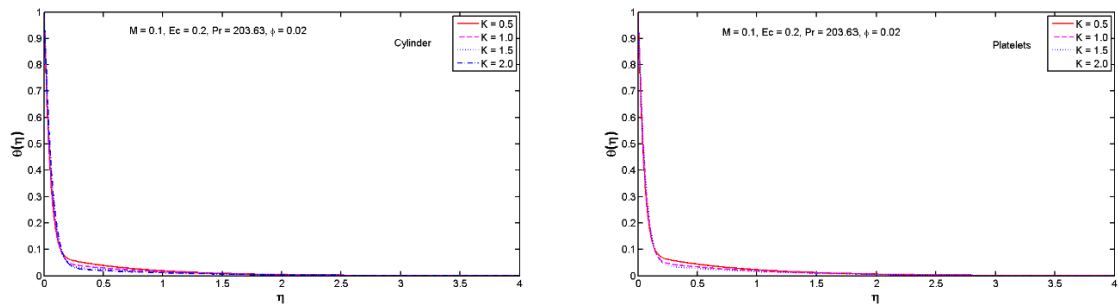


Figure 6(a-e): Effect of Magnetic Parameter (M) on Temperature Profile.



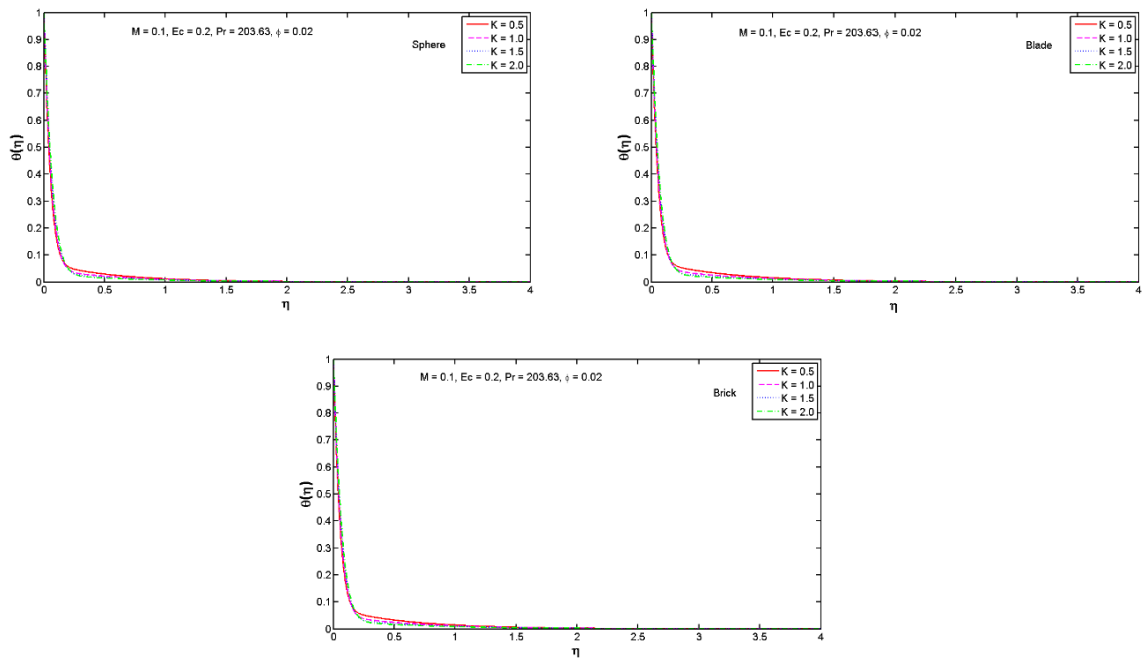


Figure 7(a-e):Effect of Slip Parameter (K) on Temperature Profile.

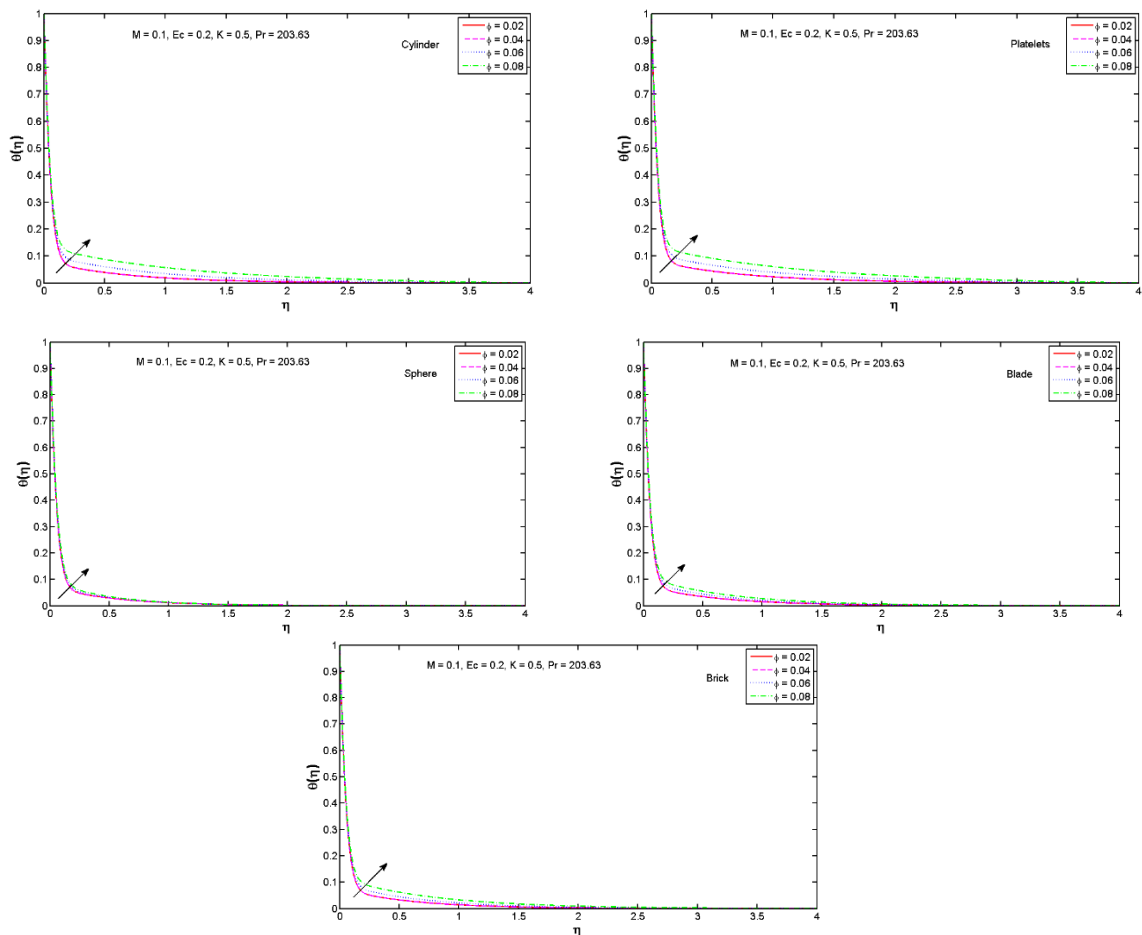


Figure 8(a-e): Influence of Volume Fraction Parameter (ϕ) on Temperature Profile.

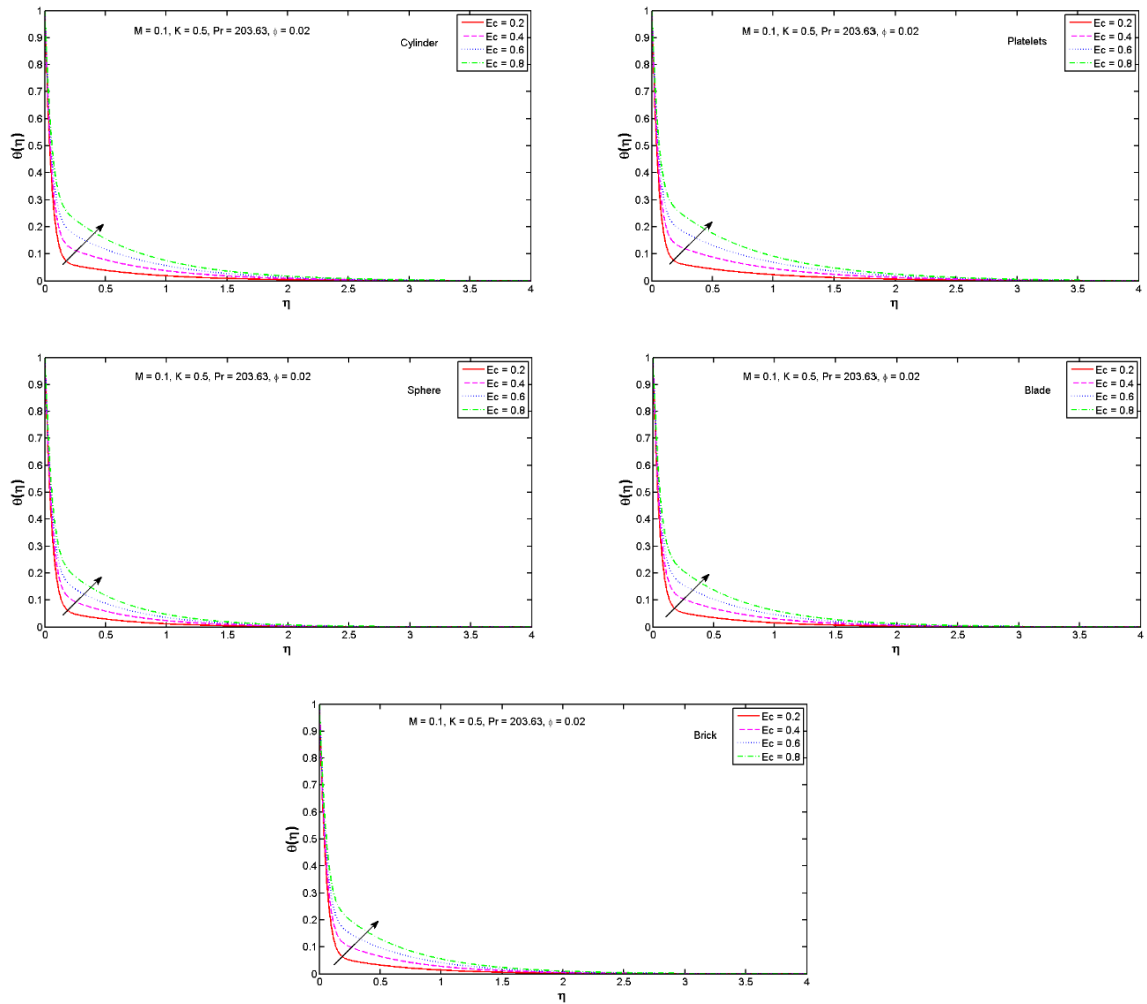


Figure 9(a-e): Effect of Eckert Number (Ec) on Temperature Profile.

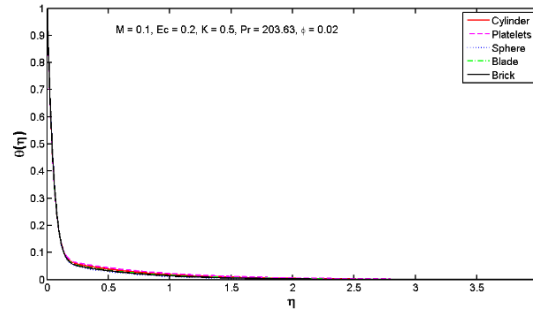


Figure 10. Variation on Temperature profile for Different shapes of nanoparticles.

In Table.3 different values of different parameter like magnetic field M and volume fraction ϕ , value of skin fraction coefficient for multi-shape Ag nanoparticle increase and for different values of slip parameter K value of skin fraction coefficient for multi-shape Ag nanoparticle decrease. In Table.4 heat transfer coefficient (Nusselt number) is calculated for different parameter like magnetic field M , volume fraction ϕ and slip parameter K . It can be observed that value of nusselt number decrease for different values of magnetic field M , slip parameter K , Eckert number (Ec) and volume fraction ϕ for multi-shapes of Ag nanoparticles.

Table 3: Numerical values of skin-friction coefficient of multi-shape nanoparticles.

M	K	ϕ	$\frac{1}{C_f Re^2}$				
			Cylinder	Platelets	Sphere	Blade	Brick
0.1	0.5	0.02	-0.91765927	-1.0515084	-0.67512884	-0.80059435	-0.75192896
0.2	-	-	-0.95074878	-1.0890802	-0.69959495	-0.82959217	-0.77918988
0.3	-	-	-0.98193453	-1.1246332	-0.72243336	-0.85680689	-0.80472821
0.4	-	-	-1.0113752	-1.1583318	-0.74381017	-0.88240459	-0.82875556
0.1	1.0	-	-0.68170189	-0.79239585	-0.48574423	-0.58632769	-0.54712794
-	1.5	-	-0.54703224	-0.64108151	-0.38284909	-0.46669704	-0.43390834
-	2.0	-	-0.45883112	-0.54067475	-0.31736311	-0.38936778	-0.36114652
-	0.5	0.04	-1.6798334	-1.8331757	-0.71220128	-1.0631935	-1.1220083
-	-	0.06	-2.4733474	-2.5315451	-0.77397548	-1.3296801	-1.5979136
-	-	0.08	-3.3928802	-3.329467	-0.83679485	-1.6267242	-2.1607114

Table 4: Numerical values of Nusselt number of multi-shape nanoparticles.

M	K	Ec	ϕ	$NuRe^{-\frac{1}{2}}$				
				Cylinder	Platelets	Sphere	Blade	Brick
0.1	0.5	0.2	0.02	17.984068	18.120664	17.61404	17.827726	17.749109
0.2	-	-	-	17.587588	17.723156	17.220928	17.432134	17.353896
0.3	-	-	-	17.207748	17.340893	16.84854	17.055225	16.97824
0.4	-	-	-	16.843572	16.972917	16.495093	16.695565	16.627225
0.1	1.0	-	-	16.580543	16.795202	16.045919	16.353792	16.243112
-	1.5	-	-	15.51869	15.764783	14.904534	15.253757	15.127592
-	2.0	-	-	14.672837	14.940748	14.020738	14.390392	14.256611
-	0.5	0.4	-	16.521286	16.552401	16.370137	16.466909	16.434873
-	-	0.6	-	15.058289	14.984138	15.126163	15.104159	15.116578
-	-	0.8	-	13.595291	13.415875	13.882189	13.741409	13.798284
-	-	0.2	0.04	17.984068	18.120664	17.61404	17.827726	17.749109
-	-	-	0.06	17.897996	17.949182	17.2424	17.616721	17.635152
-	-	-	0.08	17.583709	17.580769	16.899366	17.369294	17.458633

Concluding Remarks

This article investigated heat transfer and flow in $Ag - Nps$ with added effects like thermal radiation, joule heating, magneto-hydrodynamic (MHD), slip parameter and Viscous Dissipation over time independent stretching surfaces. Outcomes of the current study are as follows.

- **Platelet-shaped nanoparticles:** These nanoparticles exhibit a high rate of both flow and heat transfer. Their elongated shape provides a larger surface area for interaction with the surrounding fluid, facilitating efficient flow and heat exchange.
- **Spherical nanoparticles:** In contrast, nanoparticles with spherical shapes tend to have lower flow and heat transfer rates. Their smooth, symmetrical structure minimizes surface area contact with the fluid, leading to less efficient transport of heat and momentum.
- **Nusselt number:** The Nusselt number, a dimensionless parameter indicating the rate of heat transfer, decreases with increasing values of several factors. These include the magnetic parameter (M), Eckert number (Ec), slip parameter (K), and volume fraction (ϕ) of nanoparticles. This implies that these factors hinder the ability of the nanofluid to transfer heat effectively.
- **Skin friction:** The magnitude of the skin friction, a measure of the viscous force acting on the fluid's surface, increases with increasing values of the magnetic parameter (M) and volume fraction(ϕ). This signifies a stronger drag force against the flow. Conversely, the skin friction reduces for higher values of the slip parameter(K), as the slip phenomenon allows the fluid to slide more easily past the surface. Further advancements in the field will shed more light on this complex topic. By investigating the interplay of various physical factors at the nano-scale, scientists can delve deeper into the intricate relationship between nanoparticle flow, heat transfer, and Joule heating. This improved understanding can lead to the development of materials and technologies with remarkable thermal management capabilities.

References

- [1] S. Choi and J. Eastman, "Enhancing thermal conductivity of fluids with nanoparticles," *Argonne Natl. Lab.(ANL), Argonne, (United States)*, 1995.
- [2] J. A. Eastman, S. U. S. Choi, S. Li, W. Yu, and L. J. Thompson, "Anomalously increased effective thermal conductivities of ethylene glycol-based nanofluids containing copper nanoparticles," *Appl. Phys. Lett.*, vol. 78, no. 6, 2001, doi: 10.1063/1.1341218.
- [3] S. Nadeem and C. Lee, "Boundary layer flow of nanofluid over an exponentially stretching surface," *Nanoscale Res. Lett.*, vol. 7, pp. 1–6, 2012, doi: 10.1186/1556-276X-7-94.
- [4] K. Rafique, Z. Mahmood, S. Saleem, S. M. Eldin, and U. Khan, "Impact of nanoparticle shape on entropy production of nanofluid over permeable MHD stretching sheet at quadratic velocity and viscous dissipation," *Case Stud. Therm. Eng.*, vol. 45, no. January, p. 102992, 2023, doi: 10.1016/j.csite.2023.102992.
- [5] S. Bibi, Z. Elahi, and A. Shahzad, "Impacts of different shapes of nanoparticles on SiO₂nanofluid flow and heat transfer in a liquid film over a stretching sheet," *Phys. Scr.*, vol. 95, no. 11, 2020, doi: 10.1088/1402-4896/abbc9d.
- [6] K. Sharma and S. Gupta, "Viscous Dissipation and Thermal Radiation effects in MHD flow of Jeffrey Nanofluid through

- Impermeable Surface with Heat Generation/Absorption,” *Nonlinear Eng.*, vol. 6, no. 2, pp. 153–166, 2017, doi: 10.1515/nleng-2016-0078.
- [7] H. Upreti, A. K. Pandey, and M. Kumar, “MHD flow of Ag-water nanofluid over a flat porous plate with viscous-Ohmic dissipation, suction/injection and heat generation/absorption,” *Alexandria Eng. J.*, vol. 57, no. 3, pp. 1839–1847, Sep. 2018, doi: 10.1016/J.AEJ.2017.03.018.
- [8] M. Hemmat Esfe, “The Investigation of Effects of Temperature and Nanoparticles Volume Fraction on the Viscosity of Copper Oxide-ethylene Glycol Nanofluids,” vol.62, p. 1, 2018, doi: 10.3311/PPCh.9741.
- [9] E. V. Timofeeva, J. L. Routbort, and D. Singh, “Particle shape effects on thermophysical properties of alumina nanofluids,” *J. Appl. Phys.*, vol. 106, no. 1, 2009, doi: 10.1063/1.3155999.
- [10] T. Hayat, M. Qasim, and Z. Abbas, “Radiation and mass transfer effects on the magnetohydrodynamic unsteady flow induced by a stretching sheet,” *Zeitschrift fur Naturforsch. - Sect. A J. Phys. Sci.*, vol. 65, no. 3, pp. 231–239, 2010, doi: 10.1515/ZNA-2010-0312/HTML.
- [11] L. Godson, B. Raja, D. Lal, and W. SE, “Enhancement of heat transfer using nanofluids—an overview,” *Renew. Sustain. Energy Rev.*, vol. 14, no. 2, pp. 529–641, 2010.
- [12] U. Rashid and A. Ibrahim, “Impacts of Nanoparticle Shape on Al₂O₃-Water Nanofluid Flow and Heat Transfer over a Non-Linear Radically Stretching Sheet,” *Adv. Nanoparticles*, vol. 09, no. 01, 2020, doi: 10.4236/anp.2020.91002.
- [13] P. Sharma, I. H. Baek, T. Cho, S. Park, and K. B. Lee, “Enhancement of thermal conductivity of ethylene glycol based silver nanofluids,” *Powder Technol.*, vol. 208, no. 1, 2011, doi: 10.1016/j.powtec.2010.11.016.
- [14] M. H. Esfe, A. A. Arani, M. Rezaie, W. M. Yan, and A. Karimipour, “Experimental determination of thermal conductivity and dynamic viscosity of Ag-MgO/water hybrid nanofluid,” *Int. Commun. Heat Mass Transf.*, vol. 66, 2015, doi: 10.1016/j.icheatmasstransfer.2015.06.003.
- [15] T. Hayat and S. Nadeem, “Heat transfer enhancement with Ag–CuO/water hybrid nanofluid,” *Results Phys.*, vol. 7, 2017, doi: 10.1016/j.rinp.2017.06.034.
- [16] L. Godson, B. Raja, D. M. Lal, and S. Wongwises, “Experimental investigation on the thermal conductivity and viscosity of silver-deionized water nanofluid,” *Exp. Heat Transf.*, vol. 23, no. 4, 2010, doi: 10.1080/08916150903564796.
- [17] S. M. Upadhyay, C. S. K. Raju, S. Saleem, A. A. Alderremy, and Mahesha, “Modified Fourier heat flux on MHD flow over stretched cylinder filled with dust, Graphene and silver nanoparticles,” *Results Phys.*, vol. 9, 2018, doi: 10.1016/j.rinp.2018.04.038.
- [18] T. Hayat, M. I. Khan, S. Qayyum, and A. Alsaedi, “Modern developments about statistical declaration and probable error for skin friction and Nusselt number with copper and silver nanoparticles,” *Chinese J. Phys.*, vol. 55, no. 6, 2017, doi: 10.1016/j.cjph.2017.08.028.
- [19] M. N. Abrar and M. Awais, “Rheology of Alumina and Silver nanoparticles over an exponentially stretching convective wall,” *J. Comput. Theor. Nanosci.*, vol. 15, no. 4, 2018, doi: 10.1166/jctn.2018.7221.
- [20] S. T. Hussain, S. Nadeem, and R. Ul Haq, “Model-based analysis of micropolar nanofluid flow over a stretching surface,” *Eur. Phys. J. Plus*, vol. 129, no. 8, 2014, doi: 10.1140/epjp/i2014-14161-8.
- [21] D. Srinivasacharya and P. Jagadeeshwar, “Effect of Joule heating on the flow over an exponentially stretching sheet with convective thermal condition,” *Math. Sci.*, vol. 13, no. 3, pp. 201–211, 2019, doi: 10.1007/s40096-019-0290-8.
- [22] N. S. Khashi’ie, N. M. Arifin, I. Pop, and N. S. Wahid, “Flow and heat transfer of hybrid nanofluid over a permeable shrinking cylinder with Joule heating: A comparative analysis,” *Alexandria Eng. J.*, vol. 59, no. 3, pp. 1787–1798, 2020, doi: 10.1016/j.aej.2020.04.048.
- [23] S. Riaz, N. Naheed, U. Farooq, D. Lu, and M. Hussain, “Non-similar investigation of magnetized boundary layer flow of nanofluid with the effects of Joule heating, viscous dissipation and heat source/sink,” *J. Magn. Magn. Mater.*, vol. 574, no. December 2022, p. 170707, 2023, doi: 10.1016/j.jmmm.2023.170707.
- [24] O. Ghaffarpasand, “Numerical study of MHD natural convection inside a sinusoidally heated lid-driven cavity filled with Fe₃O₄-water nanofluid in the presence of Joule heating,” *Appl. Math. Model.*, vol. 40, no. 21–22, pp. 9165–9182, 2016, doi: 10.1016/j.apm.2016.05.038.
- [25] K. Ganesh Kumar, N. G. Rudraswamy, B. J. Gireesha, and M. R. Krishnamurthy, “Influence of nonlinear thermal radiation and viscous dissipation on three-dimensional flow of Jeffrey nano fluid over a stretching sheet in the presence of Joule heating,” *Nonlinear Eng.*, vol. 6, no. 3, pp. 207–219, 2017, doi: 10.1515/nleng-2017-0014.
- [26] N. S. Khashi’ie, N. M. Arifin, and I. Pop, “Magnetohydrodynamics (MHD) boundary layer flow of hybrid nanofluid over a moving plate with Joule heating,” *Alexandria Eng. J.*, vol. 61, no. 3, pp. 1938–1945, 2022, doi: 10.1016/j.aej.2021.07.032.
- [27] S. K. Khan, “Heat transfer in a viscoelastic fluid flow over a stretching surface with heat source/sink, suction/blowing and radiation,” *Int. J. Heat Mass Transf.*, vol. 49, no. 3–4, pp. 628–639, 2006, doi: 10.1016/j.ijheatmasstransfer.2005.07.049.
- [28] U. Hayat and A. Shahzad, “Analysis of heat transfer and thin film flow of Au–Np over an unsteady radial stretching sheet,” *Numer. Heat Transf. Part A Appl.*, vol. 84, no. 11, pp. 1338–1351, 2023, doi: 10.1080/10407782.2023.2175746.
- [29] S. Saleem, M. Qasim, A. Alderremy, and S. Noreen, “Heat transfer enhancement using different shapes of Cu nanoparticles in the flow of water based nanofluid,” *Phys. Scr.*, vol. 95, no. 5, p. 055209, 2020, doi: 10.1088/1402-4896/ab4ffd.
- [30] L. Shampine, J. Kierzenka, and M. Reichelt, “Solving boundary value problems for ordinary differential equations in MATLAB with bvp4c,” *Tutor. Notes*, vol. 75275, no. 1, pp. 1–27, 2000, [Online]. Available: http://200.13.98.241/~martin/irq/tareas1/bvp_paper.pdf
- [31] U. Hayat, S. Shaiq, A. Shahzad, R. Khan, M. Kamran, and N. A. Shah, “The effect of particle shape on flow and heat transfer of Ag-nanofluid along stretching surface,” *Chinese J. Phys.*, vol. 85, no. 1, pp. 708–721, 2023, doi: 10.1016/j.cjph.2023.02.008.